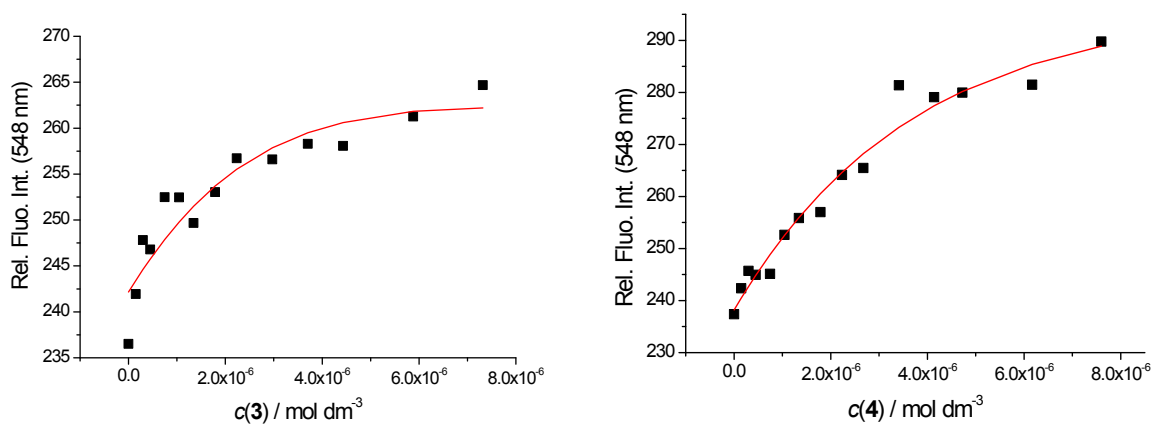


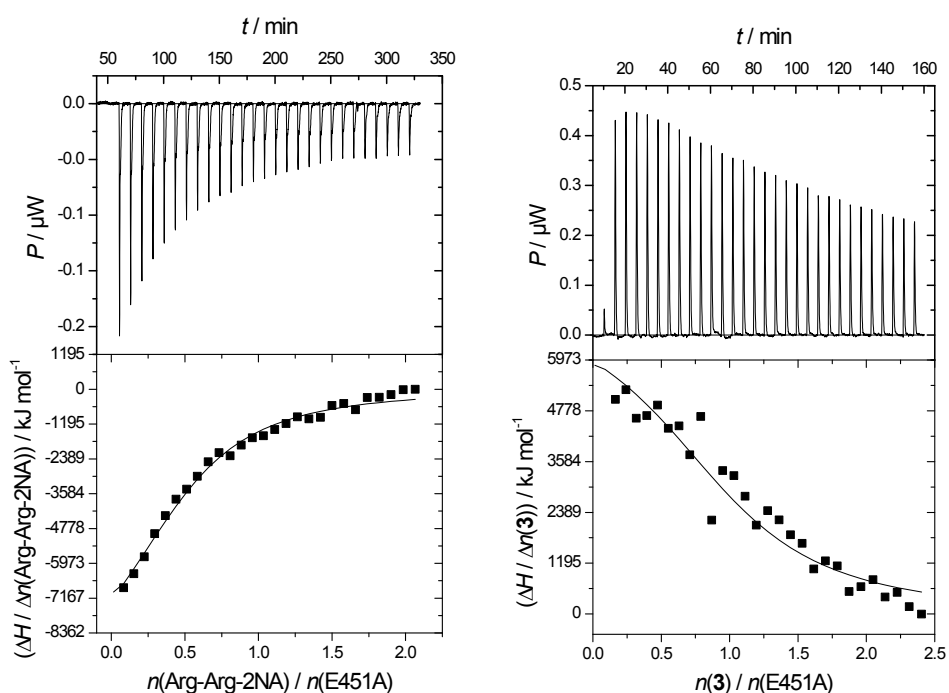
Guanidiniocarbonyl-pyrrole -aryl conjugates as inhibitors of human dipeptidyl peptidase III: combined experimental and computational study

Josipa Matic^a, Filip Šupljika^a, Nora Tir^a, Patryciusz Piotrowski^b, Carsten Schmuck^b, Marija Abramić^a, Ivo Piantanida^{a*}, Sanja Tomić^{a*}

Titration of hDDP III with 1, 3 and 4



Scheme S1. Fluorimetric titration of hDPP III mutant E451A with 3 (LEFT) and 4 (RIGHT): $c(\text{enzyme}) = 2 \times 10^{-6}$ M, $\lambda_{\text{exc}} = 350$ nm, $\lambda_{\text{em}} = 548$ nm; done at pH = 7.4, 20 mM tris-HCl buffer.



Scheme S2. ITC titrations of hDPP III mutant E451A with Arg-Arg-2NA (LEFT) and 3 (RIGHT); $c(\text{enzyme}) = 2.5 \times 10^{-6}$ M. Done at pH = 7.4, 20 mM tris-HCl buffer.

Molecular modelling

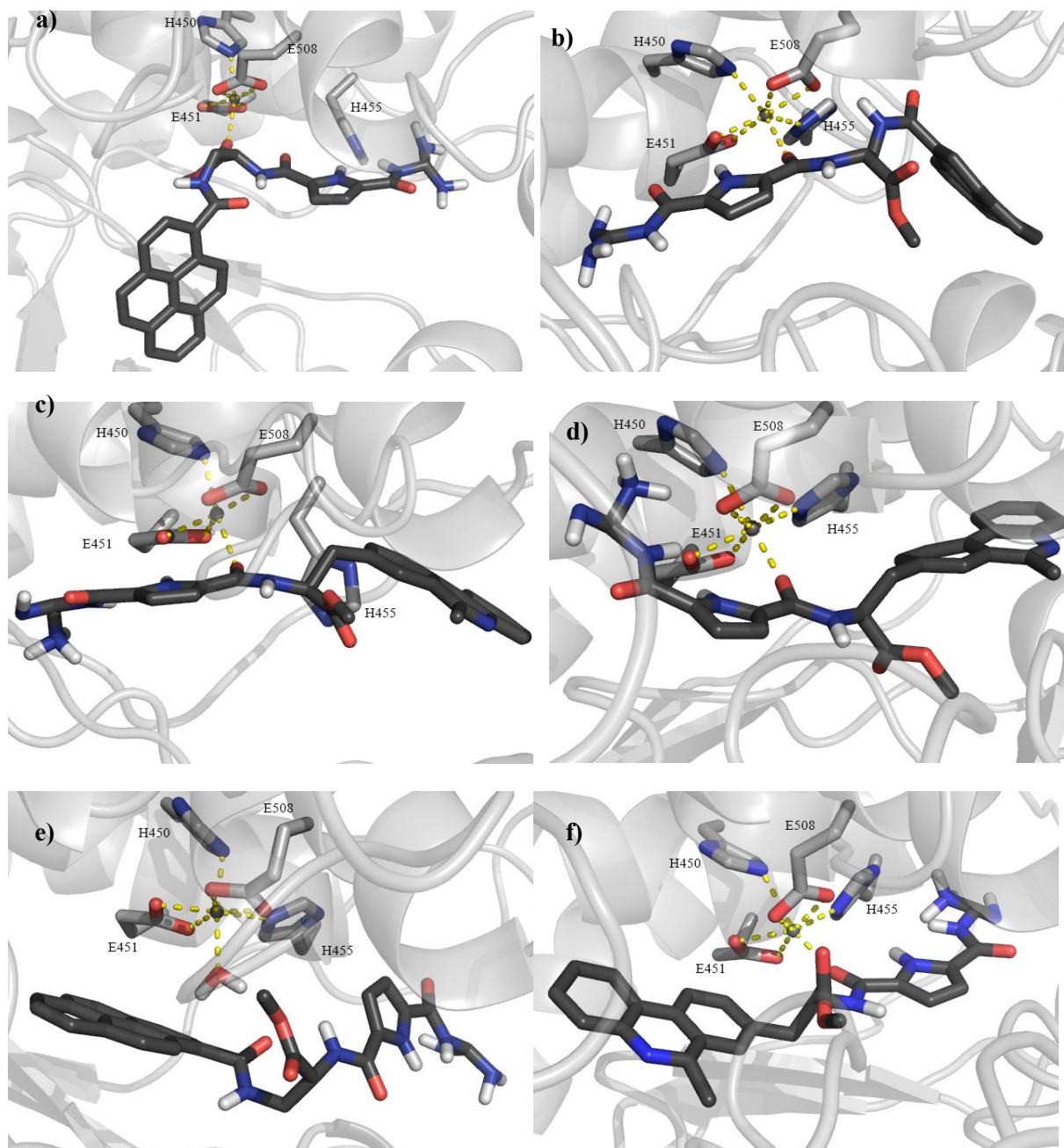


Figure S1. Structure of the initial complexes: a) cWT_{MD}-2(AD1), b) cWT_{MD}-2(AD2), c) cWT_{MD}-3(AD), d) cWT-2(AD), e) cWT-2, f) cWT-3.

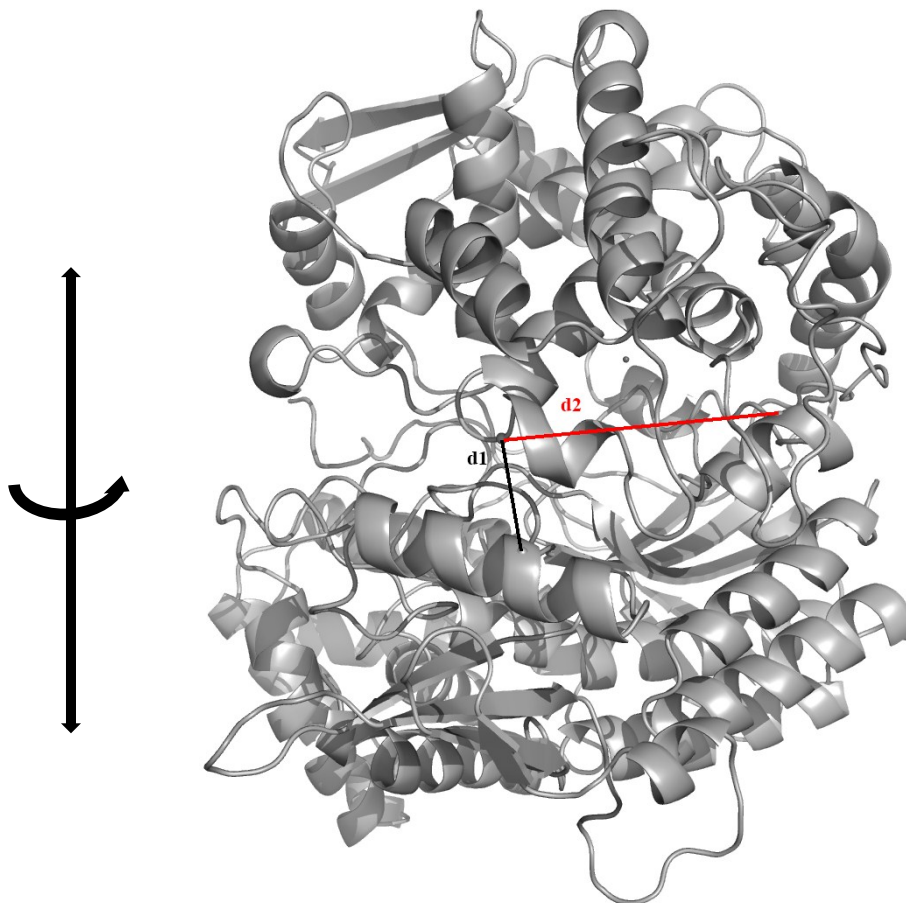


Figure S2. Distances between D186-S500 and Q400-S500 α atoms, d_1 and d_2 , respectively, describe the mutual position of the two DPP III domains. Their values for the most relevant h.DPP III structures are given in the table below:

	oWT	cWT	cWT_{MD}
$d_1(\text{D186-S500}) / \text{\AA}$	38.5	11.6	17.0
$d_2(\text{Q400-S500}) / \text{\AA}$	25.2	20.9	8.2

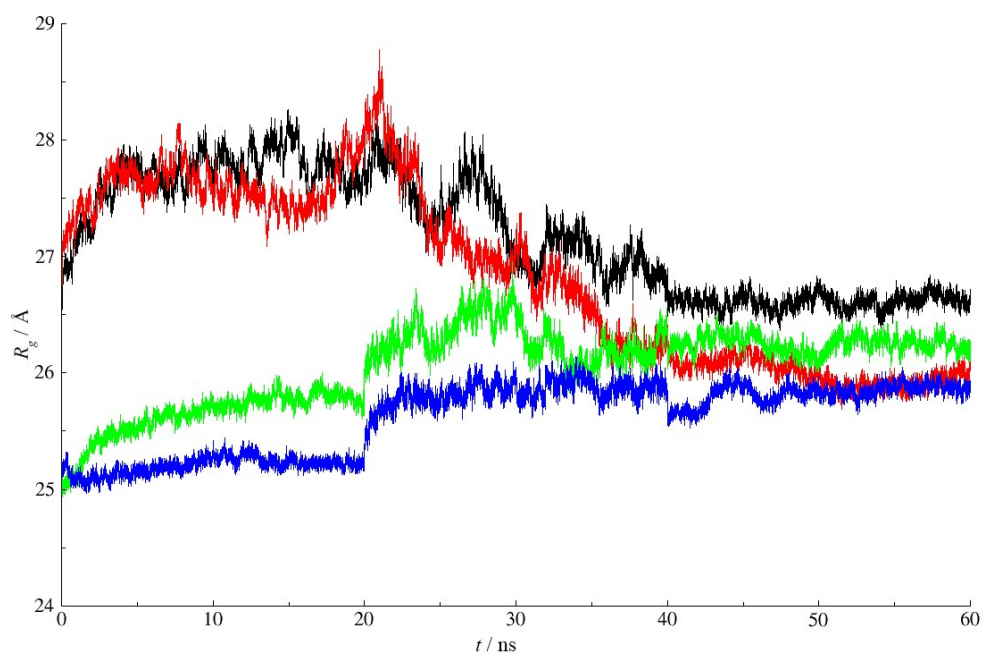
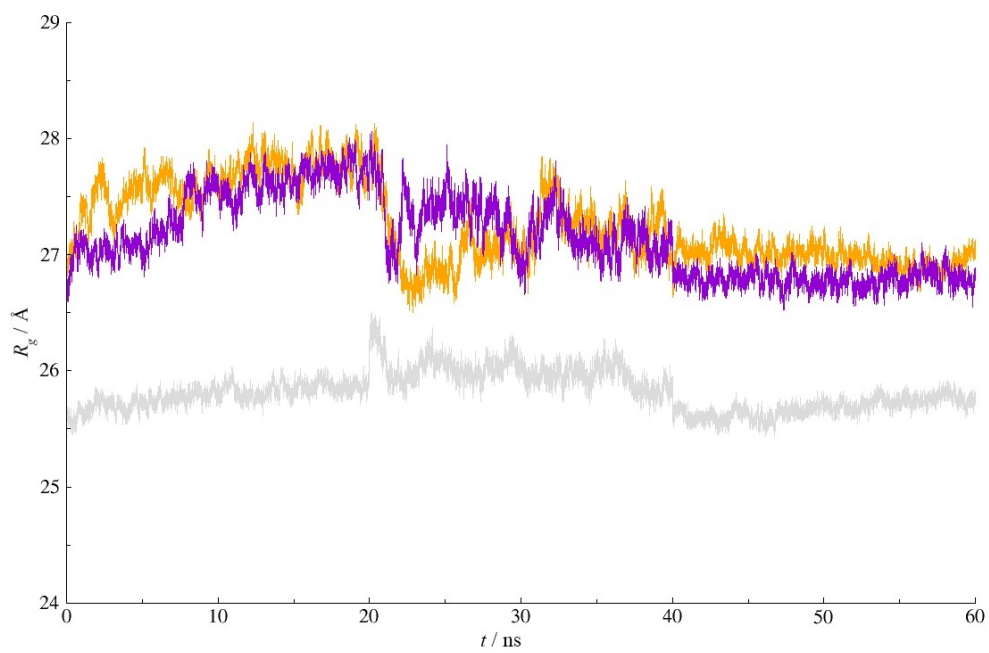


Figure S3. Radius of gyration traced during simulations of the h.DPP III – 2 complexes (TOP) and h.DPP III – 3 complexes (BOTTOM).

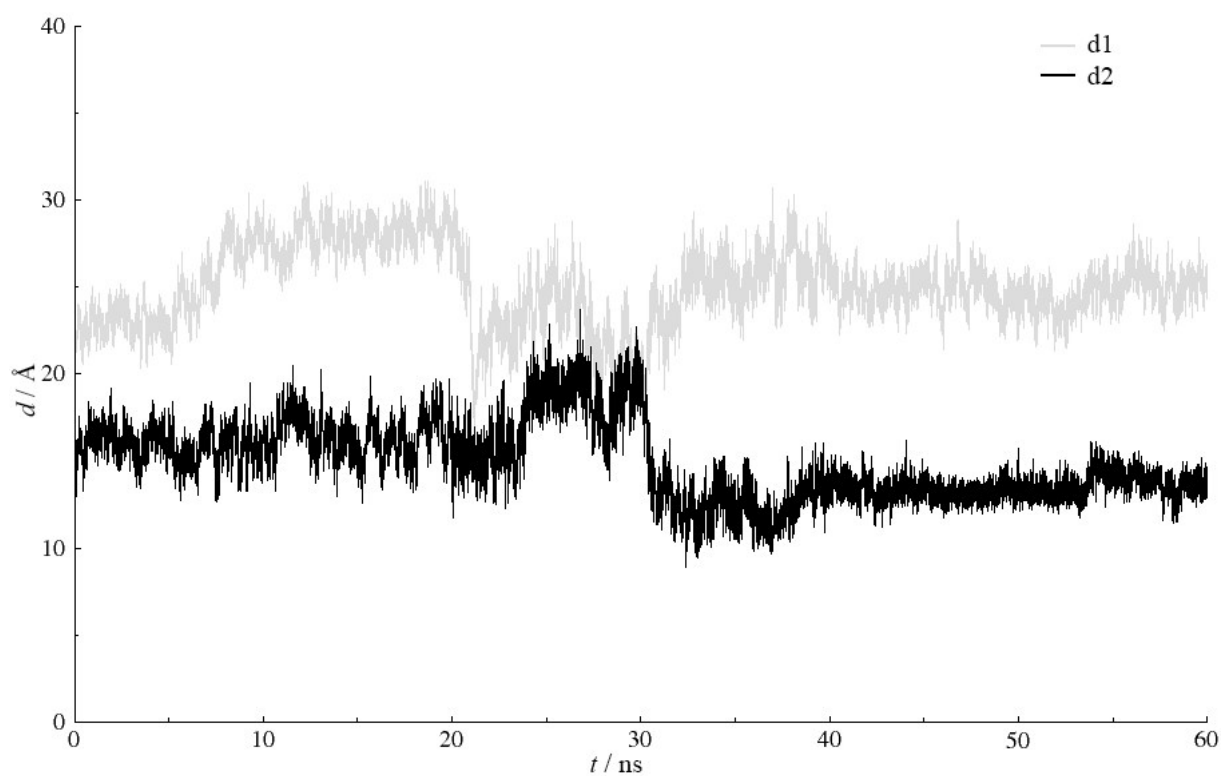
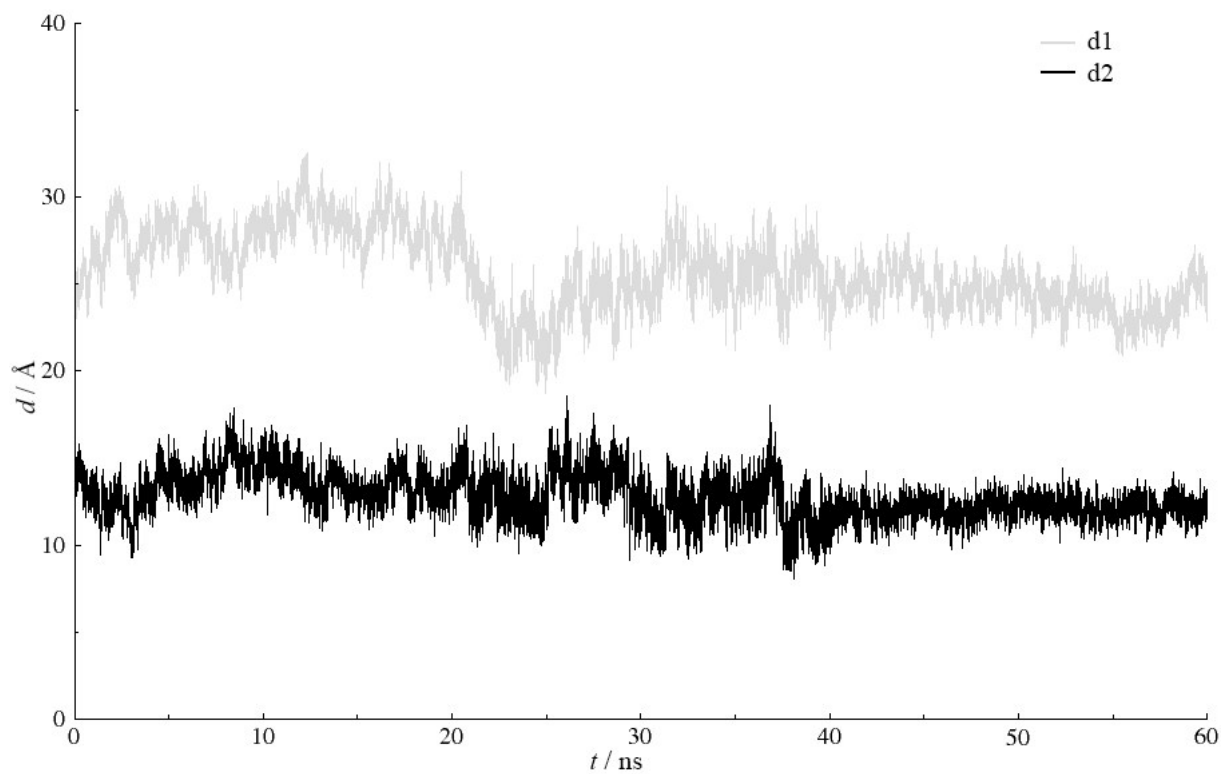


Figure S4 Profile of distances d_1 and d_2 determined during simulations of the $cWT_{MD-2}(AD1)$ (TOP) and $cWT_{MD-2}(AD2)$ (BOTTOM) complexes.

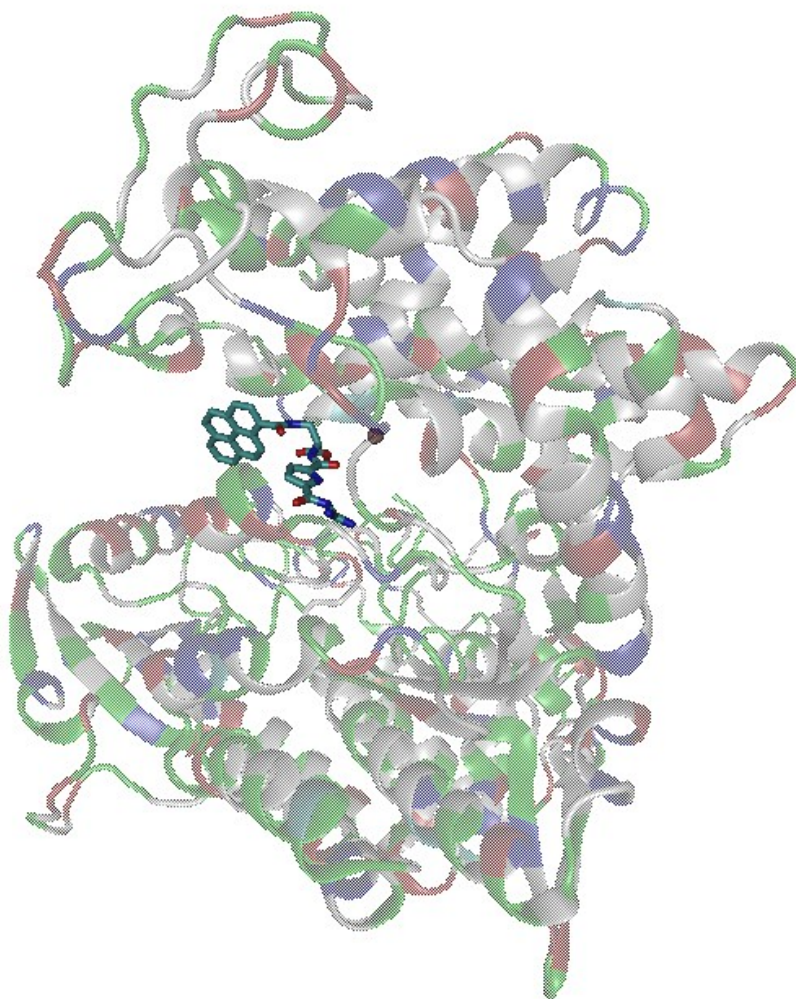


Figure S5 cWT_{MD}-2(AD1) complexes. Inhibitor, **2** is given in stick representation, and h.DPP III is represented as ribbon.

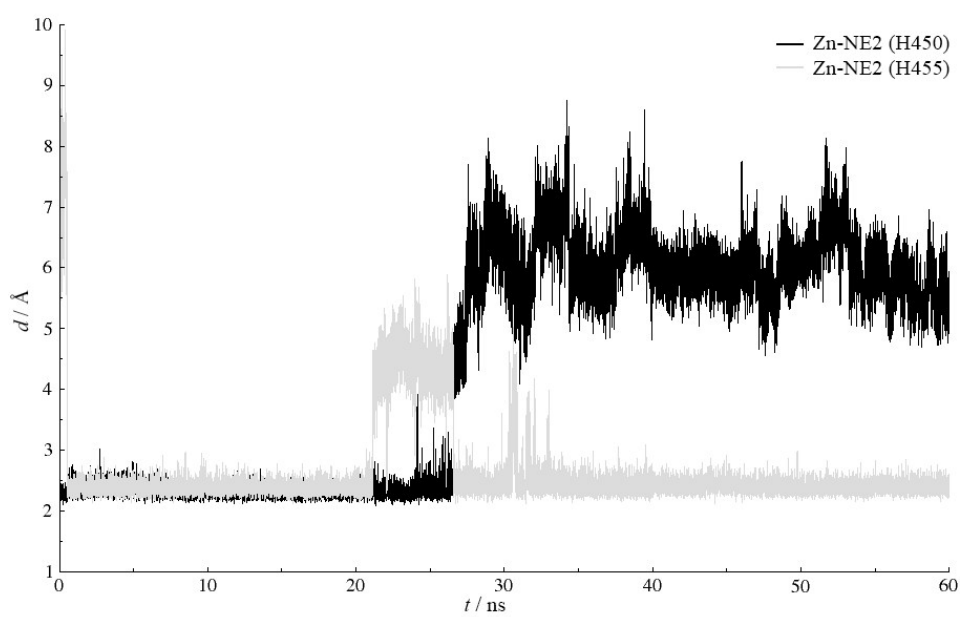


Figure S6 Changes in Zn²⁺ coordination noticed during simulations of cWT_{MD}-2(AD),

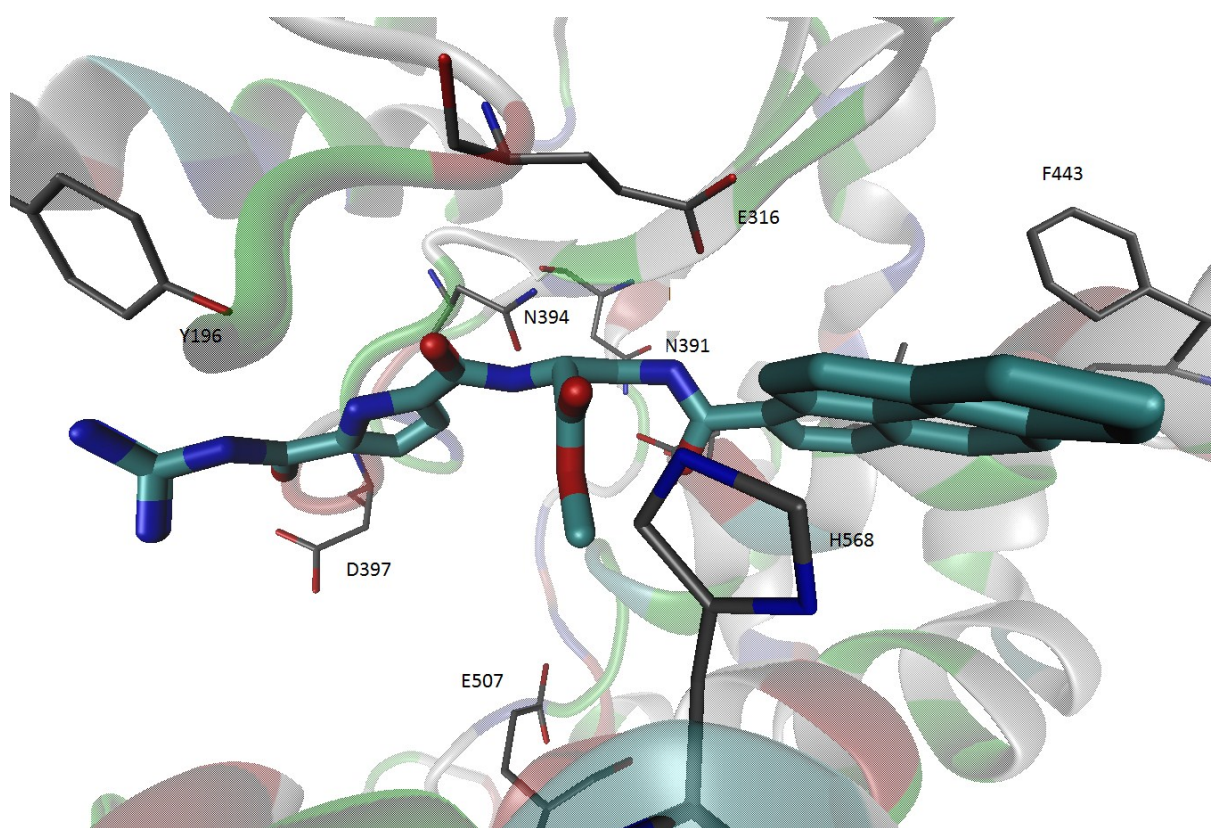
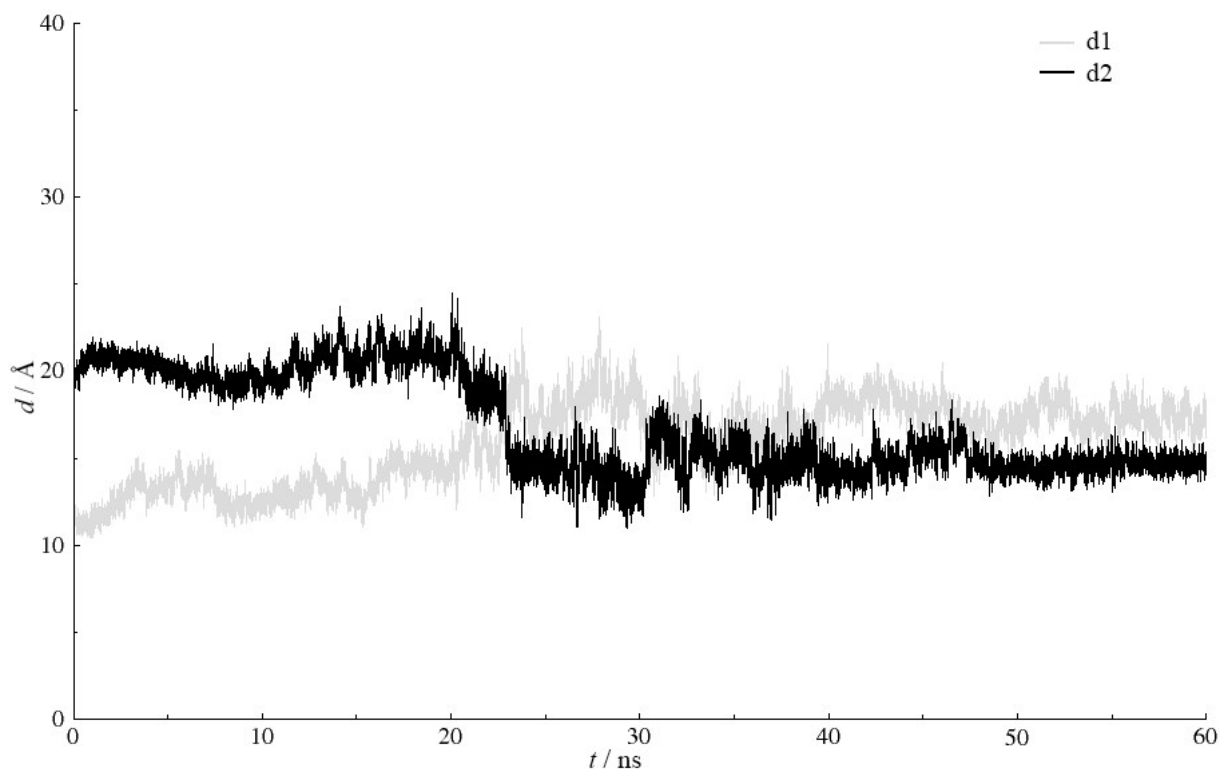
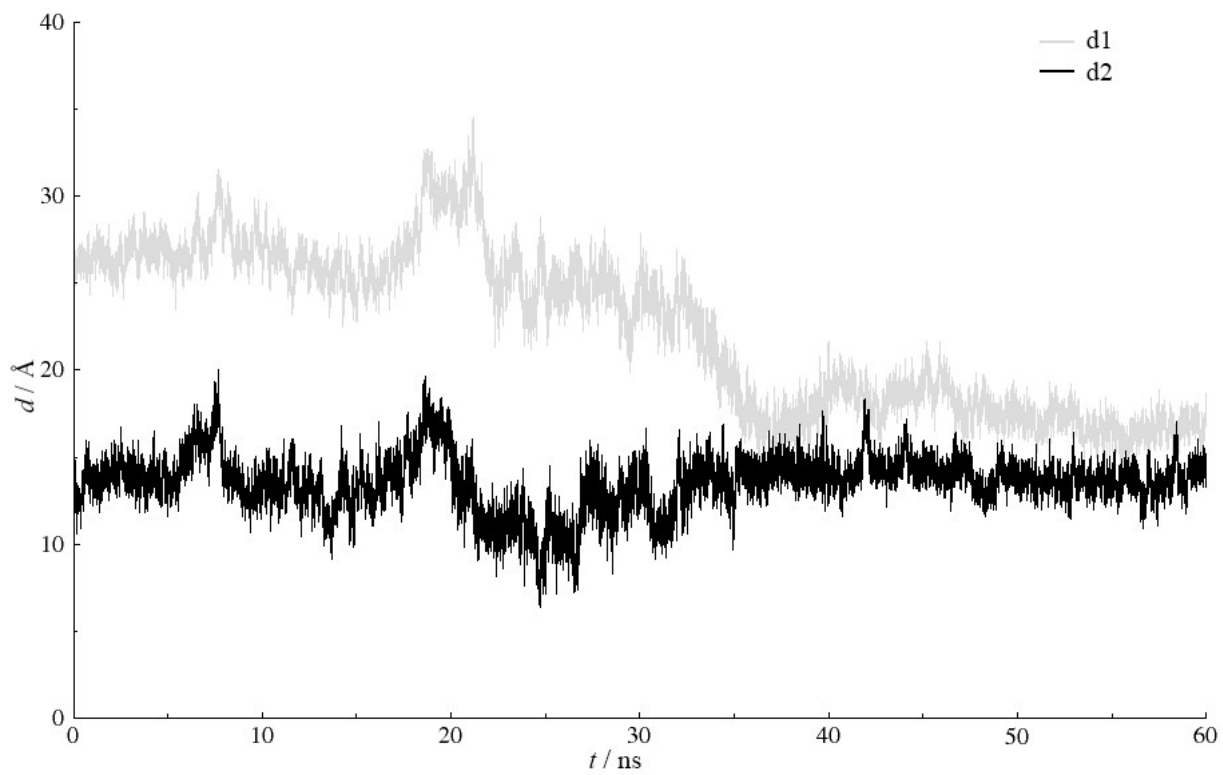


Figure S7 Interactions between **2** and the amino acid residues from the DPP III active site inter-domain cleft.



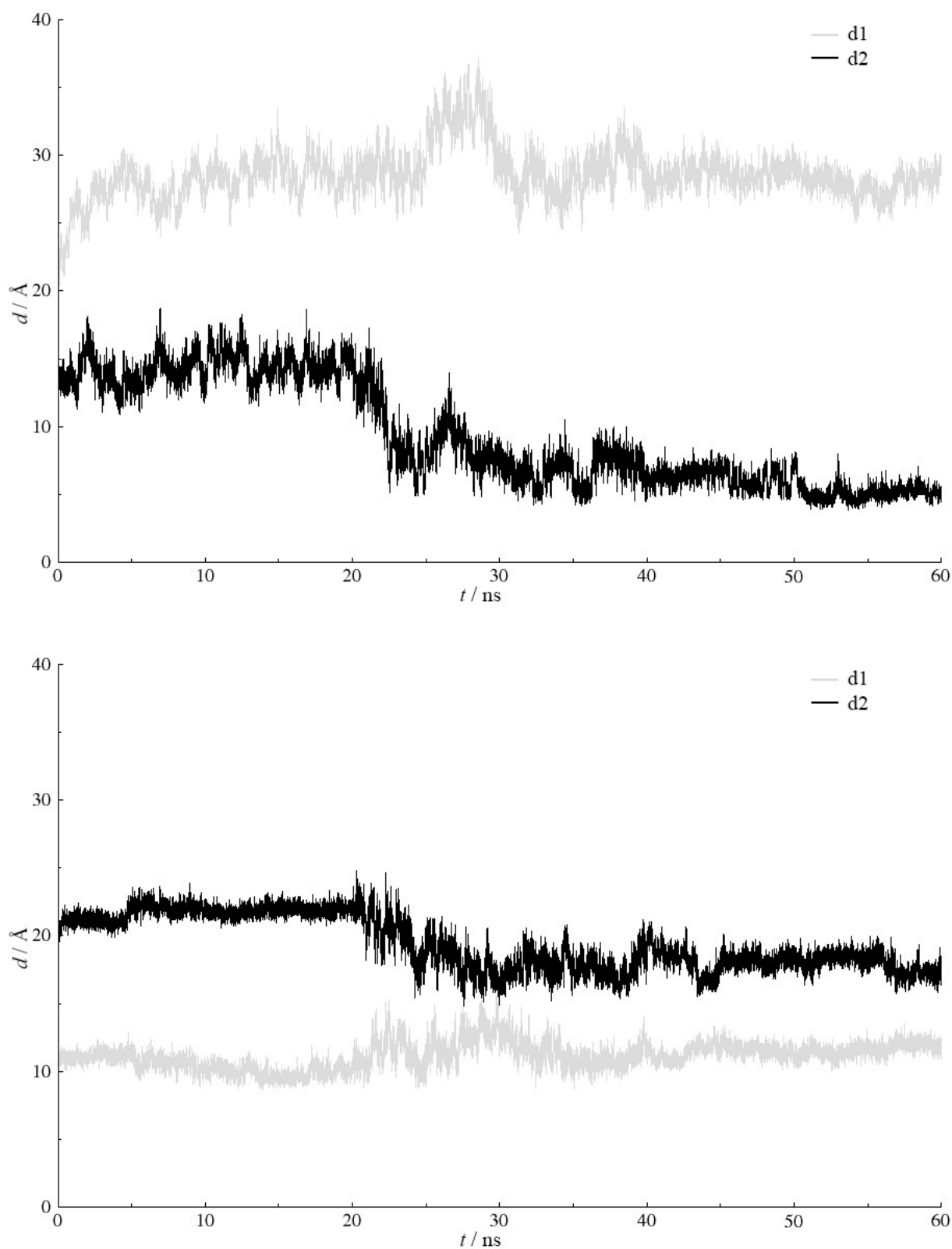


Figure S8 Profile of distances d_1 and d_2 determined during simulations of cWT_{MD}-3(AD), cWT-3(AD), cWT_{MD}-3 and cWT-3 complexes, from top to bottom, respectively.

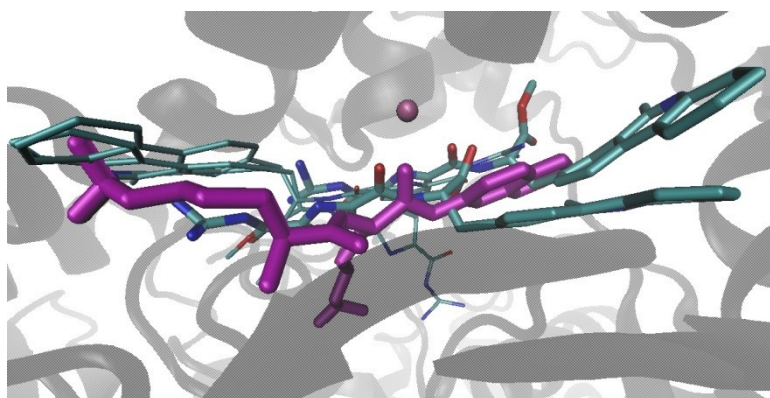


Figure S9 Alignment of the inhibitor **3** and RRNA bound into the h.DPP III interdomain cleft. cWT_{MD}-**3**(AD) and cWT-**3**(AD) are represented by thin sticks, while cWT_{MD}-**3** and cWT-**3** are represented by thick sticks. Arg-Arg-NA is given in magenta colored stick representation.

Table S1 Components of the MMGBSA and MMPBSA binding free energies

MMGBSA			
	$(\Delta G_{gas} \pm \sigma) /$ kcal mol ⁻¹	$(\Delta G_{solv} \pm \sigma) /$ kcal mol ⁻¹	$(\Delta G_{tot} \pm \sigma) /$ kcal mol ⁻¹
cWT-2	-387 ± 13	353 ± 11	-34 ± 5
cWT-2'	-471 ± 12	442 ± 10	-29 ± 5
cWT-3	160 ± 12	-179 ± 11	-19 ± 4

MMPBSA			
	$(\Delta G_{gas} \pm \sigma) /$ kcal mol ⁻¹	$(\Delta G_{solv} \pm \sigma) /$ kcal mol ⁻¹	$(\Delta G_{tot} \pm \sigma) /$ kcal mol ⁻¹
cWT-2	-227 ± 7	181 ± 7	-46 ± 4
cWT-2'	-259 ± 6	218 ± 6	-40 ± 4
cWT-3	56 ± 6	-77 ± 8	-21 ± 5

The binding free energies were calculated using coordinates generated during the last 5 ns of MD simulations. Dielectric constant for enzyme was set either to 2 (PB calculations) or 1 (GB calculations), and for solvent to 80. Ionic strength was 0.1 mM. Nonpolar solvation energy was calculated from solvent accessible surface (SASA), $\Delta_{sol}H_{np} = \gamma SASA + \beta$, wherein γ , surface tension is $0,0378 \text{ kJ mol}^{-1} \text{ \AA}^{-2}$, and *offset*, β , $-0,5692 \text{ kJ mol}^{-1}$.